Int. J. Heat Mass Transfer. Vol. 33, No. 10, pp. 2237–2245, 1990
Printed in Great Britain

0017-9310/90 $3.00+0.00
© 1990 Pergamon Press plc

On the thermocapillary instabilities in a liquid layer heated from below

D. A. GOUSSIS† and R. E. KELLY

Mechanical, Aerospace, and Nuclear Engineering Department, University of California, Los Angeles, Los Angeles, CA 90024, U.S.A.

(*Received* 25 *July* 1989 *and in final form* 3 *January* 1990)

Abstract—The instability due to thermocapillary forces at the free surface of a horizontal liquid layer heated from below is studied. It is shown that there exist two distinct mechanisms by which thermal effects can lead to a destabilizing thermocapillary force. One mechanism is associated with the modification of the basic temperature by the deformation of the free surface and generates long wavelength disturbances. The other mechanism is associated with the interaction of the basic temperature with the perturbation velocity field and generates disturbances the wavelength of which is of the same order as the layer depth. When the temperature difference across the layer is small, instability occurs when the layer is sufficiently thin. For larger temperature differences, thin and thick layers are unstable, while layers of moderate depth are stable. When the temperature difference is beyond a certain value, there is no depth that will render the layer stable. These results, as well as others describing the stability of the layer, are obtained in a clear manner by use of non-dimensional parameters which are appropriate for a comparison of theoretical results with experimental data.

1. INTRODUCTION

A LIQUID layer heated from below can be subject to an instability caused by forces at the free surface which are due to surface tension variations produced by temperature gradients. This type of instability was first examined by Pearson [1] who neglected the buoyancy effects and assumed the free surface to be nondeformable. Scriven and Sterling [2] extended this analysis by considering the effects of surface deformation. They showed that disturbances of sufficiently large wavelength were always unstable, while disturbances of sufficiently small wavelength exhibited the behavior discussed by Pearson. The instability at large wavelengths was attributed to the omission from consideration of gravity in restoring the free surface. Smith [3] concluded that gravity becomes important only at small wave numbers and for thin layers of very viscous liquids. In all the analyses above, the marginal state was assumed to be stationary. For the thermocapillary instability, the validity of this assumption cannot be proven analytically as for the Rayleigh–Benard problem. Vidal and Acrivos [4] provided numerical evidence that the marginal state for the problem considered by Pearson is indeed stationary. A similar proof for the marginal state was given by Takashima [5] for the problem examined by Smith.

In the problem of thermocapillary instability in a liquid layer heated from below the free surface of which is allowed to deform, there are some questions which are still unanswered. In the case where the free surface is nondeformable, it is well known that the mechanism giving rise to the thermocapillary force is associated with the convective interaction of the perturbation velocity field and the basic temperature. For this mode, instability occurs for sufficiently thick layers [1]. However, for the deformable case, an increase of the layer's depth will reinforce the stabilizing effect of gravity on the surface waves. It is therefore reasonable to ask whether there exist depths that are small enough so as not to allow the interaction of perturbation velocity with the basic state temperature leading to instability and, at the same time, large enough to stabilize the surface waves. An answer to this question cannot be obtained from Smith's analysis due to the particular set of non-dimensional parameters used. In that set, the layer depth appeared in more than one non-dimensional parameter.

Another aspect which has not yet been resolved is the following. For surface waves to exist, the free surface must be allowed to deform. In addition, surface waves usually have large wavelengths so that the effects of convection are negligible. Therefore, the mechanism which is responsible for sustaining the surface deformation under the action of thermocapillary forces should not be associated with the interaction of the perturbation velocity with the basic state temperature.

In this paper, the issues discussed above will be addressed along with some additional ones which arise in the course of the analysis. First the governing equations will be derived and then the results will be presented.

† Present address: Mechanical and Aerospace Engineering Department, Princeton University, Princeton, NJ 08540, U.S.A.

NOMENCLATURE

g gravity
h heat transfer coefficient
H layer depth
k wave number, $[k_x^2+k_y^2]^{1/2}$
k_x wave number in x-direction
k_y wave number in y-direction
K thermal conductivity
N amplitude of free surface deflection
p perturbation pressure
P basic state pressure
t time
T basic state temperature
ΔT^* temperature difference, $T_w^*-T_o^*$
$\mathbf{u}$ perturbation velocity field, $[u, v, w]$
x, y, z spatial coordinates.

Greek symbols
α growth rate
η free surface deflection
θ perturbation temperature
Θ amplitude of perturbation temperature
κ thermal diffusivity
μ dynamic viscosity
ν kinematic viscosity
ρ density
σ surface tension
Φ amplitude of perturbation velocity.

Non-dimensional parameters
Bi Biot number, $(h/K)(2\nu^2/g)^{1/3}$
Bo Bond number, $(\rho/\sigma)(4\nu^4 g)^{1/3}$
M Marangoni number, $-(\mathrm{d}\sigma/\mathrm{d}T)(\Delta T^*/\rho\nu)(2/\nu g)^{1/3}$
Pr Prandtl number, ν/κ
χ Archimedes number, $gH^3/2\nu^2$.

Subscripts
c critical conditions
i imaginary part
o ambient conditions
r real part
w wall conditions.

Superscript
* dimensional quantities.

2. THE GOVERNING EQUATIONS

For the scaling of the governing equations a set of non-dimensional parameters will be used which is appropriate for a comparison of the theoretical results with experimental data. In this set, each of the physical parameters with which one might control the experiment (i.e. the depth of the layer, or the temperature difference) appears in only a single non-dimensional parameter. As will be shown later, this set, which was introduced in ref. [6], is a very useful tool in the physical interpretation of the numerical results.

Consider a horizontal liquid layer on a heated plate. Let x and y denote the two coordinates that are parallel to the plate and let z be the coordinate perpendicular to the plate. It is assumed that all physical properties, except the surface tension, are constant. The effects of compressibility and viscous dissipation are ignored. The surface tension is taken to depend on temperature in the form

$$\sigma = \sigma_o + \left[\frac{\mathrm{d}\sigma}{\mathrm{d}T}\right]_o (T^* - T_o^*). \tag{1}$$

The velocity vector $\mathbf{u}^*$, temperature T^*, pressure P^*, and time t^*, are scaled as

$$\mathbf{u}^* = \left(\frac{\nu}{H}\right)\mathbf{u}, \quad T^* = \Delta T^*(T+\theta)+T_w^*$$

$$\Delta T^* = (T_w^* - T_o^*)$$

$$P^* = \rho g H P + \rho\left(\frac{\nu}{H}\right)^2 p, \quad t^* = \left(\frac{H^2}{\nu}\right)t.$$

With these assumptions and scalings, the linearized non-dimensional stability equations (continuity, momentum, and energy equations) for a three-dimensional disturbance become [7]

$$u_x + v_y + w_z = 0 \tag{2a}$$

$$u_t = -p_x + \nabla^2 u \tag{2b}$$

$$v_t = -p_y + \nabla^2 v \tag{2c}$$

$$w_t = -p_z + \nabla^2 w \tag{2d}$$

$$\theta_t + w\,DT = \frac{1}{Pr}\nabla^2\theta. \tag{2e}$$

The above equations are supplemented with boundary conditions at the wall and the free surface. At the wall we have the no-slip, non-permeable, and isothermal conditions

$$u = v = w = \theta = 0, \quad \text{at } z = 1. \tag{3a–d}$$

At the free surface the normal and shear stress conditions, the heat balance, and the kinematic condition are

$$-2\chi\eta\,DP - p + w_z + \left(\frac{2\chi^{1/3}}{Bo}\right)\nabla^2\eta = 0, \quad \text{at } z = 0 \tag{4a}$$

$$u_z + w_x = \frac{M}{Bi}\theta_{zx}, \quad \text{at } z = 0 \tag{4b}$$

$$v_z + w_y = \frac{M}{Bi}\theta_{zy}, \quad \text{at } z = 0 \tag{4c}$$

$$\theta_t = Bi\chi^{1/3}(\eta DT + \theta), \quad \text{at } z = 0 \qquad (4d)$$

$$\eta_t = w, \quad \text{at } z = 0. \qquad (4e)$$

The basic state is expressed by $T = 1 - z$ and $P = z$. Substituting in the equations above the following expressions for the perturbation quantities:

$$(w, \theta, \eta) = [\Phi(z), \Theta(z), N] \exp[\mathrm{i}(k_x x + k_y y - \alpha t)] \qquad (5)$$

the governing equations become

$$(D^2 - k^2)^2\Phi + \mathrm{i}\alpha(D^2 - k^2)\Phi = 0 \qquad (6a)$$

$$(D^2 - k^2)\Theta + Pr(\mathrm{i}\alpha\Theta - \Phi DT) = 0 \qquad (6b)$$

$$\Phi(1) = D\Phi(1) = \Theta(1) = 0 \qquad (6c–e)$$

$$(D^3 - 3k^2 D)\Phi(0) + \mathrm{i}\alpha D\Phi(0) + 2k^2\left(DP(0) + \frac{k^2}{Bo\chi^{2/3}}\right)N = 0 \qquad (6f)$$

$$(D^2 - k^2)\Phi(0) - k^2\frac{M}{Bi}D\Theta(0) = 0 \qquad (6g)$$

$$D\Theta(0) = Bi\chi^{1/3}[NDT(0) + \Theta(0)] \qquad (6h)$$

$$N = \frac{\mathrm{i}\Phi(0)}{\alpha}. \qquad (6i)$$

Assuming that the marginal state is stationary ($\alpha = 0$), the system (6a)–(6i) yields the following analytic solution [1, 7]:

$$\Phi = 2[(A_2 + kB_1) + 2kB_2 z]\cosh(kz) + 2[(B_2 + kA_1) + 2kA_2 z]\sinh(kz) \qquad (7a)$$

$$\Theta = Pr\left\{\left[\frac{A_0}{Pr} + A_1 z + A_2 z^2\right]\cosh(kz) + [B_0 + B_1 z + B_2 z^2]\sinh(kz)\right\} \qquad (7b)$$

where

$$A_0 = \frac{QR_1}{M\chi^{1/3}Pr} - 1, \quad A_1 = \frac{Q}{8}R_2, \quad A_2 = \frac{Q}{8}R_1$$

$$B_0 = -\frac{Q}{8k}\left[R_2 - 8\frac{Bi}{M\,Pr}R_1\right]$$

$$B_1 = -\frac{Q}{8k}R_1, \quad B_2 = -\frac{Q\sinh^2 k}{8k^3}$$

$$Q = 2\chi\left(1 + \frac{k^2}{Bo\chi^{2/3}}\right)$$

$$R_1 = \frac{\cosh k - k}{k^3}, \quad R_2 = \frac{\sinh^2 k + 2k^2}{k^4}.$$

The marginal state is described by the relation

$$2\chi\left(\frac{F_1}{M\chi^{1/3}} - Pr F_2\right)\left(1 + \frac{k^2}{Bo\chi^{2/3}}\right) = F_3 \qquad (8)$$

where

$$F_1 = 8k(\sinh k\cosh k - k)(Bi\chi^{1/3}\sinh k + k\cosh k)$$

$$F_2 = \sinh^3 k - k^3\cosh k$$

$$F_3 = 8k^5\cosh k.$$

Table 1. Values of the non-dimensional parameters at different temperatures for water [14]

	T(°C)				
	10	15	20	25	30
$M/\Delta T$	6.02	7.25	9.03	10.80	12.55
$(\chi/H^3)\times 10^{-12}$	2.87	3.77	4.86	6.16	7.64
$Bo \times 10^4$	6.54	5.50	4.68	4.04	3.53
$(Bi/h)\times 10^4$	5.13	4.58	4.12	3.76	3.47
Pr	9.45	8.09	7.01	6.13	5.43

$[\Delta T]$ = °C, $[H]$ = m, $[h]$ = cal m^{-2} s^{-1} K^{-1}.

Table 2. Convergence and accuracy test: $k = 3$, $M = 30$, $Pr = 7$, $Bo = 4.7\times 10^{-4}$, $Bi = 5$

N	χ_n	χ_a
6	105.0375143	
8	7.3532696	
10	7.3961195	
12	7.3962176	
14	7.3962165	7.3962165

N, number of terms in the Chebyshev series.
Subscripts: 'n', numerical solution; 'a', analytical solution.

The stability problem examined here is characterized by the parameters χ, M, Pr, Bi, and Bo. Since there is a large number of parameters, a complete investigation over the entire parameter space becomes a consuming and probably an unnecessary task. Therefore, the analysis will consider values of the parameters that are either physically meaningful or important in affecting the shape of stability boundaries. Table 1 presents typical values of these parameters for water at different temperatures.

The system of differential equations (6a)–(6i) was solved numerically using the Tau method [8], where the eigenfunctions Φ and Θ were expanded in Chebyshev series. The resulting singular quadratic eigenvalue problem was transformed [9, 10] into a regular one and then it was solved by the QZ algorithm [11]. The agreement of the computed solution with the analytic solution, equations (7a), (7b) and (8), at the marginal state was excellent [12]. As Table 2 indicates, ten terms in the Chebyshev series provided sufficient accuracy.

3. RESULTS

Numerical solutions obtained for various sets of parameters indicate that the marginal state is indeed stationary. A typical set of values of α for the first ten modes of a neutral disturbance is presented in Table

Table 3. Values of α for the ten first modes of a neutral disturbance: $k = 3$, $M = 53$, $Pr = 7$, $Bo = 10^{-4}$, $Bi = 10$, $\chi = 7.1193$

Mode	α_r	α_i
10	0	−64.762
9	0	−56.231
8	0	−34.622
7	0	−28.322
6	0	−22.151
5	1014.968	−17.171
4	−1014.968	−17.171
3	0	−13.048
2	0	−5.475
1	0	0

3, where mode 1 corresponds to the marginal state. For all modes, except modes 4 and 5, the real part of α is zero. Modes 4 and 5 represent waves traveling at equal speeds but in opposite directions and correspond to surface waves which exist even in the absence of the thermocapillary forces [12]. These two modes are always stable and disappear when $Bo = 0$.

Since the marginal state is stationary, the stability boundaries are given by equation (8). Some neutral curves that arise for different values of Bo are presented in Fig. 1. For sufficiently small Bond numbers there exist two separate unstable regions. The region in the upper-right part of the figure is bounded by a neutral curve (corresponding to $Bo = 0.4$) of the type found by Pearson who neglected surface deformation. This curve yields a minimum at $\chi = \chi_{c,u}$ and $k = k_{c,u}$, the latter being always nonzero. The two branches of this neutral curve tend to infinity as $k \to k_1$ or $k \to k_2$, where k_1 and k_2 are determined by the following relation obtained from equation (8) by considering the limit $\chi \to \infty$

$$\frac{8Bi}{M\,Pr} = \frac{\sinh^3 k - k^3 \cosh k}{k \sinh k(\sinh k \cosh k - k)}. \tag{9}$$

Equation (9) shows that as $(M\ Pr)/Bi \to \infty$, $k_1 \to 0$ and $k_2 \to \infty$. As the ratio $(M\ Pr)/Bi$ decreases from infinity, k_1 and k_2 approach each other while, as will be shown later, $\chi_{c,u}$ increases. Finally, as $(M\ Pr)/Bi \to 32.073$ from above, k_1 and $k_2 \to 3.015$, while $\chi_{c,u} \to \infty$. When

$$\frac{M\,Pr}{Bi} < 32.073 \tag{10}$$

an unstable region on the upper part of the χ–k plane does not exist.

The unstable region that exists on the lower left part of the χ–k plane in Fig. 1 is bounded by a neutral curve which bifurcates from the $k = 0$ axis at a value of χ determined by equation (8), which in the $k \to 0$ limit reduces to

$$\chi^{2/3} = \frac{3M}{4(1+Bi\,\chi^{1/3})}. \tag{11}$$

Such an unstable region is obtained only when the free surface is allowed to deform. This is shown from equation (8) which in the $Bo \to 0$ limit (non-deformable surface) becomes

$$F_1 = M\,Pr\,\chi^{1/3} F_2. \tag{12}$$

Using a small wave number expansion, the above equation yields

$$\chi^{1/3} = \frac{1+O(k^4)}{-Bi+O(k^2)} \tag{13}$$

which clearly shows that there is no neutral curve bifurcating from the $k = 0$ axis. For $Bo > 0$, the lower neutral curve yields a maximum at, say, $\chi = \chi_{c,1}$ and $k = k_{c,1}$. Except for some cases that will be discussed later, $k_{c,1} = 0$. Figure 1 shows that, as the Bond number increases, the two unstable regions approach each other until they form a single unstable region.

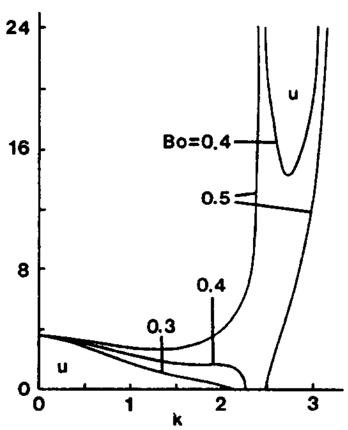

Fig. 1. Neutral curves for different values of Bo and $M = 50$, $Pr = 7$, $Bi = 10$. u, unstable region.

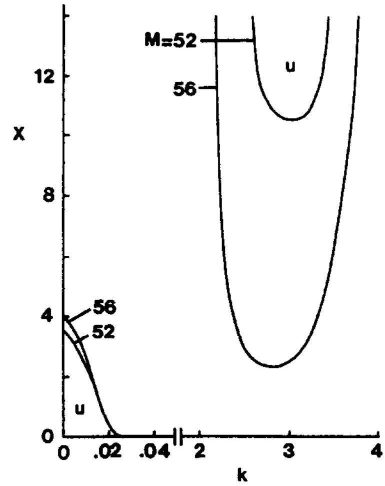

Fig. 2. Neutral curves for different values of M and $Pr = 7$, $Bi = 10$ ($M_{min} = 45.7$), $Bo = 10^{-4}$. u, unstable region.

Figure 2 shows the effects of Marangoni number in the case where the Bond number is small. When M is sufficiently small, $\chi_{c,u} > \chi_{c,1}$ so that there is a range of values of χ for which the flow is stable. As M increases, $\chi_{c,u}$ decreases while $\chi_{c,1}$ increases. After a certain value

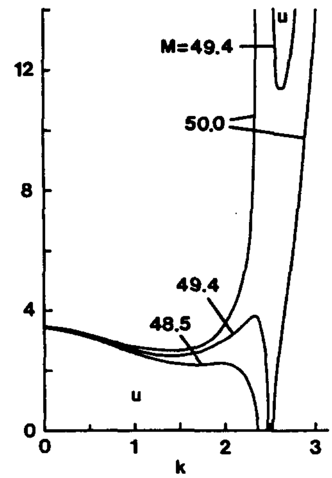

FIG. 3. Neutral curves for different values of M and $Pr = 7$, $Bi = 10$ ($M_{min} = 45.7$), $Bo = 0.5$. u, unstable region.

of M, $\chi_{c,u} < \chi_{c,l}$ so that the layer is unstable for all values of χ. As Fig. 2 shows, this happens while the two unstable regions remain separate. However, when the Bond number is sufficiently large, the two unstable regions approach each other, as M increases, forming a single region. This is shown in Fig. 3, where it is also shown that $\chi_{c,l}$ might occur at non-zero values of k. The variation of χ_c with M is shown in Fig. 4. When $M < M_{min}$, where according to equation (10)

$$M_{min} = 32.073\frac{Bi}{Pr} \qquad (14)$$

an unstable region in the upper part of the χ–k plane does not exist. In this case, there is only one critical value of χ, corresponding to the lower unstable region, above which value the layer is stable. As M increases beyond M_{min}, an unstable region is formed in the upper part of the χ–k plane, so that there are two critical values of χ. Now, there is a definite range of values of χ for which the layer is stable. With further increase of M, this range decreases until the layer becomes unstable for all values of χ. As Fig. 4 shows,

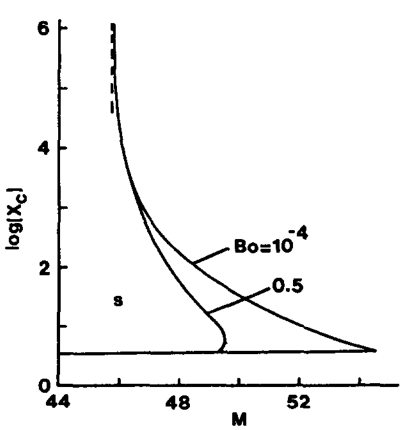

FIG. 4. The variation of χ_c with M for two values of Bo and $Pr = 7$, $Bi = 10$ ($M_{min} = 45.7$). ---, M_{min}; s, stable region.

the effect of varying M is more pronounced on $\chi_{c,u}$ than on $\chi_{c,l}$. Increasing values of the Bond number tend to limit the stable region mainly by decreasing $\chi_{c,u}$. This effect is restricted to small values of $\chi_{c,u}$ while larger ones remain unaffected, tending to infinity as $M \to M_{min}$.

As Fig. 2 indicates, there is a range of values of χ for which both very large and short wavelength disturbances are unstable. It turns out that the growth rate α_i of the latter form is much larger than that of the former form [12]. Therefore, it is expected that, in that case, short wavelength disturbances will manifest themselves first.

Decreasing values of Bi and increasing values of Pr have the same effects as increasing values of M [12], i.e. destabilizing. The only difference is that $\chi_{c,l}$ (when it occurs at $k_{c,l} = 0$) is independent of Pr, while it depends on Bi. As with M_{min}, there is a maximum value of Bi and a minimum value of Pr, defined by

$$Bi_{max} = \frac{M\,Pr}{32.073}, \quad Pr_{min} = 32.073\frac{Bi}{M} \qquad (15)$$

above and below which, respectively, an $\chi_{c,u}$ does not exist so that the layer becomes unstable only when $\chi < \chi_{c,l}$.

Instability in the two regions of the χ–k plane is due to thermocapillary forces. Apparently, the mechanisms involved for growth of the disturbance in these regions are different. A necessary condition for these forces to arise is that the free surface be nonisothermal. Considering real quantities and neglecting the contribution from the basic state profile which is a constant, the temperature variation at the free surface is given by the expression

$$[N\,DT(0) + \Theta(0)]\cos\phi\exp(\alpha_i t) \qquad (16)$$

where $\phi = k_x x + k_y y$, and α_i is the growth rate. The two terms in brackets denote the variations which come from the basic temperature field due to surface deformation and from the perturbation temperature. In order to examine the relative contribution of these two terms in the temperature variation (16), N was set equal to unity and $\Theta(0)$ was evaluated along the neutral curves. With this normalization equation (16) becomes

$$[1 + \Theta(0)]\cos\phi\exp(\alpha_i t). \qquad (17)$$

The variation of $\Theta(0)$ with k for the $Bo = 0.3$ neutral curves of Fig. 1 are presented in Fig. 5. Along the neutral curve which bifurcates from the $k = 0$ axis $-1 < \Theta(0) \leqslant 0$, while along the type of neutral curve found by Pearson $\Theta(0) > 1$. Along both neutral curves $1 + \Theta(0) > 0$, so that the trough of the wave ($\phi = 0°$) represents a hot spot and the peak of the wave ($\phi = 180°$) represents a cold spot. The surface tension gradient that is thus established (the surface tension has a minimum at the trough and a maximum at the peak), generates a surface flow from the trough to the peak.

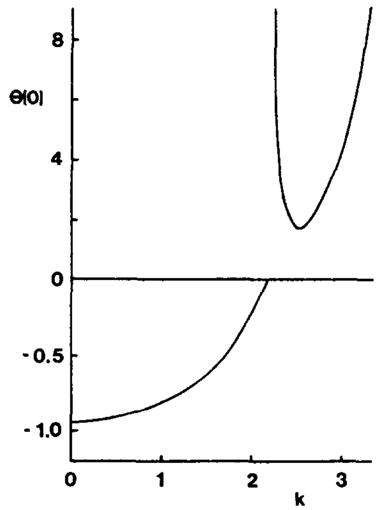

FIG. 5. The variation of Θ(0) along the neutral curve. $M = 50$, $Pr = 7$, $Bi = 10$, $Bo = 0.3$.

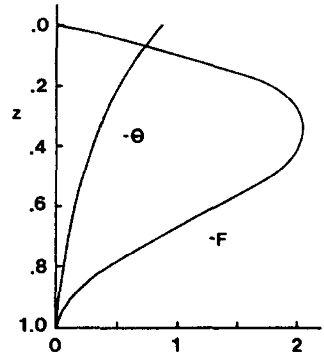

FIG. 6. The profiles of Θ and F at the lower neutral curve. $\chi = 1.45$, $k = 1$, $M = 50$, $Pr = 7$, $Bi = 10$, $Bo = 0.3$.

Although the driving force and the manifestation of instability are the same in the two unstable regions, the results shown in Fig. 5 indicate that the effects of the perturbation temperature at the free surface on the stability of the layer are different. In the lower unstable region $\Theta(0) < 0$, so that the perturbation temperature tends to cool (heat) the hot (cold) spot, thus stabilizing the flow. Therefore, in this region, the surface tension gradient necessary for instability is a direct result of the modification of the basic state temperature by the surface deformation. In the upper unstable region where $\Theta(0) > 0$, the perturbation temperature has the opposite effect, i.e. it tends to destabilize the layer. Moreover, since $\Theta(0) > 1$, the destabilizing influence of Θ is greater than that resulting from the modification of the basic state temperature by the free surface deformation.

The different behavior of $\Theta(0)$ in the two unstable regions can be explained by examining the behavior of the perturbation temperature inside the liquid layer. Since $NDT(0)+\Theta(0) > 0$ along both neutral curves when $N > 0$, equation (6h) indicates that at the hot (cold) spot heat leaves (enters) the free surface. As a result, the perturbation temperature profile has a positive (negative) slope under the hot (cold) spot. In Figs. 6 and 7 the profile of Θ is presented for a disturbance in the lower and upper neutral curves of Fig. 1, respectively. For the lower neutral curve, Fig. 6 shows that heat is transferred across the film basically by conduction. Therefore, the positive (negative) slope of the perturbation temperature that exists under the hot (cold) spot prevails throughout the layer. As a result, since $\Theta(1) = 0$, $\Theta(0) < 0$. For the upper neutral curve, Fig. 7 shows that an interior hot (cold) spot is formed below the hot (cold) spot of the free surface. This interior hot (cold) spot, which is a result of the convective motion, is strong enough that it heats (cools) the free surface by conduction. For both neutral curves, Figs. 6 and 7 indicate that, in agreement with Davis and Homsy [13], under the cold spot at the free surface there is an upward motion of fluid, while under the hot spot the opposite occurs.

From the discussion above it is clear that there exist two mechanisms by which energy is supplied from the basic state to the disturbance. The first mechanism takes place at the free surface and is associated with the effect of the free surface deformation on the basic state temperature. This mechanism is represented by the term $NDT(0)$ in the heat balance (6h). The second mechanism takes place in the bulk of the fluid and is associated with the interaction of the perturbation velocity field with the basic state temperature. This mechanism is represented by the term FDT in the energy equation (6b).

The nature of these two mechanisms determines the region in the χ–k plane where each dominates. When $k \ll 1$, as the analytical solution (7) shows, $F = O(k^2)$ while Θ and N are both order one quantities. In this limit, the energy equation (6b) shows that the effects of convection are small, so that the dominant mechanism for energy transfer to the disturbance is the one which is associated with the surface deformation. In addition, equation (6f) shows that what mainly opposes the surface deformation is gravity while the effects of surface tension are negligible. Therefore, instability will occur when the balance between the thermocapillary forces and the forces due to the hydrodynamic forces turns in favor of the former.

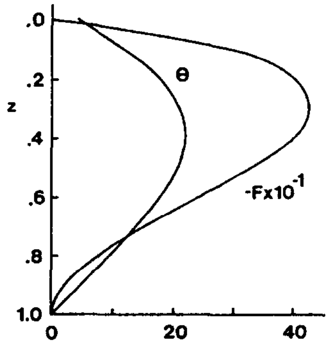

FIG. 7. The profiles of Θ and F at the upper neutral curve. $\chi = 14.47$, $k = 2.75$, $M = 50$, $Pr = 7$, $Bi = 10$, $Bo = 0.3$.

This balance is expressed by equation (8), which in the $k \ll 1$ limit and in dimensional form becomes

$$H^2 \rho g = \frac{\frac{3}{2}\left[-\frac{d\sigma}{dT}\right]_o \Delta T}{1+\frac{hH}{K}}. \tag{18}$$

If the depth of the layer is less than that indicated by the above expression, the layer is unstable at least with respect to large wavelength disturbances. For disturbances of somewhat smaller wavelength, the restoring force due to surface tension becomes important. As a result, a smaller depth (i.e. hydrodynamic pressure), is required for neutral stability. This is shown in all the stability diagrams, where the neutral curve which bifurcates from the $k = 0$ axis has initially a negative slope.

Surface deformation is also important when $\chi^{1/3} \ll 1$ and $k = O(1)$. In this case $F = O(\chi^{1/3})$, while Θ and N are both order one quantities. As in the previous case, the effects of convection are small and the instability is associated with the modification of the basic temperature profile by the surface deformation. However, what now opposes the deformation is surface tension while the effects of gravity are negligible. The effects of surface tension increase as the wave number increases. Therefore, there is a value of the wave number beyond which the flow is stable. This is shown from equation (8), which in the $\chi^{1/3} \to 0$ limit and in dimensional form becomes

$$\left[-\frac{d\sigma}{dT}\right]_o \Delta T = \sigma_o \frac{\sinh k \cosh k - k}{k}. \tag{19}$$

When the surface tension is sufficiently large, the neutral curve, which bifurcates from the $k = 0$ axis, reaches the $\chi = 0$ axis at small wave numbers (see Figs. 1 and 2) so that the critical wave number $k_{c,1}$ is zero. However, as the surface tension decreases, this neutral curve extends into a region where both χ and k are order one quantities. As we will see next, for such values of χ and k convection becomes important so that the perturbation temperature at the free surface has now a destabilizing influence. This influence, though less important than that of the surface deformation, might offset the increased stabilizing influence of surface tension, so that a larger force due to hydrostatic pressure will be required for neutral stability. Therefore, as Figs. 1 and 3 show, for small values of the surface tension the critical wave number $k_{c,1}$ can be nonzero.

When $\chi \gg 1$ and $k = O(1)$, equation (7) shows that F and Θ are both order one quantities while $N = O(\chi^{-1})$. The governing equations then show that the effects of convection become important, while the effects of surface deformation are negligible. In fact as equation (7) shows, this type of instability occurs even in the absence of surface deformation. The different physical aspects which are associated with this type of instability all show-up in condition (14) for this mode to exist, which in dimensional form yields

$$\left[-\frac{d\sigma}{dT}\Delta T\right]\frac{\rho c_p}{\mu h} > 32.073. \tag{20}$$

In the inequality above the terms in brackets is a measure of the thermocapillary forces, while ρc_p is a measure of the effects of convection in extracting energy from the basic state. Large values of both these quantities are favorable for instability. The dynamic viscosity μ and heat transfer coefficient h are measures of the energy loss due to viscous dissipation and to the heat loss through the free surface, respectively. For instability to occur at large values of χ, the energy transfer to the disturbance and the work done by the thermocapillary forces have to be enough to overcome both these two kinds of losses.

4. CONCLUSIONS

The instability due to thermocapillary forces in a horizontal liquid layer heated from below was examined. It was shown that there exist two energy sources for the disturbance to grow. The first source is associated with the modification of the basic temperature by the deformation of the free surface, while the second source is associated with the interaction of the basic temperature with the perturbation velocity field.

Using a specific set of non-dimensional parameters, the regions in the stability diagrams where each of the energy sources dominates were completely separated. The first source can cause instability when the layer is sufficiently thin. The perturbation temperature tends to stabilize the layer. However, the main stabilizing influence for this mode comes from the gravity force which tends to suppress the deformation of the free surface. Surface tension stabilizes short wavelengths so that the instability takes the form of large wavelength disturbances. In the case where the surface tension is sufficiently small, with the reinforcement by the second energy source, the instability can take the form of relatively short wavelengths. For the instability caused by the second energy source the effects of convection are important. Therefore, it occurs at sufficiently thick layers at wavelengths which are of the order of the layer's depth. Very large wavelength disturbances are stabilized via heat loss through the surface, while very short wavelength disturbances are stabilized by viscous dissipation [12].

The role of the depth of the layer was shown to be very important. For sufficiently weak thermocapillary forces, instability might occur only when the layer is thin. For stronger forces (i.e. equation (20)), sufficiently thin and thick layers are unstable; only layers with moderate depth are stable. As the thermocapillary forces increase, the range of depths for which the layer is stable decreases. When these forces are sufficiently strong, there is no depth that will render the liquid layer stable.

The examination of the effects of the layer depth H and the derivation of equation (10) were based on a non-dimensional set of parameters in which H appears in one parameter only. Such results cannot be obtained on the basis of the sets used in previous analyses, since H appeared in more than one parameter.

The instability of the surface waves under the thermocapillary action is very important in conditions of weak gravity forces. Reducing these forces will make the first energy source more effective in causing instability, while the second source will remain unaffected. The result is that the stable region in the M–χ plane will be considerably reduced [12]. The liquid layer will be stable only when the depth is very thick and the temperature difference is small enough not to satisfy equation (20).

Acknowledgements—The support of NSF under Grant No. MEA 82-04944 is gratefully acknowledged.

REFERENCES

1. J. R. A. Pearson, On convection cells induced by surface tension, *J. Fluid Mech.* **4**, 489–500 (1958).
2. L. E. Scriven and C. V. Sterling, On cellular convection driven surface tension gradients: effects of mean surface tension and surface viscosity, *J. Fluid Mech.* **19**, 321–340 (1964).
3. K. A. Smith, On convective instability induced by surface tension, *J. Fluid Mech.* **24**, 401–414 (1966).
4. A. Vidal and A. Acrivos, Nature of the neutral state in surface tension driven convection, *Physics Fluids* **9**, 615–617 (1966).
5. M. Takashima, Surface tension driven instability in a liquid layer with a deformable free surface, *J. Phys. Soc. Japan* **50**, 2745–2753 (1981).
6. R. E. Kelly, S. H. Davis and D. A. Goussis, On the instability of heated film flow with variable surface tension, *Proc. 9th Int. Heat Transfer Conf.*, Vol. 4, pp. 1939–1942 (1986).
7. S. Sreenivasan and S. P. Lin, Surface tension driven instability of a liquid film down a heated incline, *Int. J. Heat Mass Transfer* **21**, 1517–1526 (1978).
8. D. Gottlieb and S. A. Orszag, *Numerical Analysis of Spectral Methods: Theory and Applications*. SIAM, Philadelphia (1977).
9. A. J. Pearlstein and D. A. Goussis, Efficient transformation of singular matrix eigenvalue problems, *J. Comp. Phys.* **78**, 305–312 (1988).
10. D. A. Goussis and A. J. Pearlstein, Removal of infinite eigenvalues in the generalized eigenvalue problem, *J. Comp. Phys.* **84**, 242–246 (1989).
11. C. B. Moler and G. W. Stewart, An algorithm for generalized matrix eigenvalue problems, *SIAM J. Numer. Analysis* **10**, 241–256 (1973).
12. D. A. Goussis, Instabilities of stratified film flows, Ph.D. Thesis, University of California, Los Angeles, California (1986).
13. S. H. Davis and G. M. Homsy, Energy stability theory for free surface problems: buoyancy-thermocapillary layers, *J. Fluid Mech.* **98**, 527–553 (1980).
14. D. K. Edwards, V. E. Denny and A. F. Mills, *Transfer Processes*. McGraw-Hill, New York (1979).

INSTABILITES THERMOCAPILLAIRES DANS UNE COUCHE LIQUIDE CHAUFFE PAR DESSOUS

Résumé—On étudie l'instabilité due à des forces thermocapillaires sur la surface libre d'une couche liquide horizontale chauffée par dessous. On montre qu'il existe deux mécanismes distincts par lesquels les effets thermiques peuvent conduire à une force thermocapillaire déstabilisante. Un mécanisme est associé à la modification de la température de base par la déformation de la surface libre et il génère des perturbations de grande longueur d'onde. L'autre mécanisme est associé à l'interaction de la température de base avec le champ de vitesse de perturbation et il génère des perturbations dont la longueur d'onde est du même ordre de grandeur que l'épaisseur de la couche. Quand la différence de température à travers la couche est faible, l'instabilité se produit si l'épaisseur est suffisamment fine. Pour de grandes différences de température, les couche minces ou épaisses sont instables, alors que les couches d'épaisseurs modérées sont stables. Lorsque la différence de température est supérieure à une certaine valeur, il n'y a pas d'épaisseur qui rende la couche stable. Ces résultats sont obtenus d'une façon claire en utilisant des paramètres adimensionnels qui sont appropriés pour une comparaison des résultats théoriques et des données expérimentales.

THERMOKAPILLARE INSTABILITÄTEN IN EINER VON UNTEN BEHEIZTEN FLÜSSIGKEITSSCHICHT

Zusammenfassung—Die Instabilität in einer waagerechten, von unten beheizten Flüssigkeitsschicht aufgrund thermokapillarer Kräfte an der freien Oberfläche wird untersucht. Es zeigt sich, daß es zwei ausgeprägte Mechanismen gibt, durch die thermischen Einflüsse zu einer destabilisierenden thermokapillaren Kraft führen können. Einer der Mechanismen ist mit der Veränderung der Grundtemperatur durch die Deformation der freien Oberfläche verbunden, er erzeugt langwellige Störungen. Der andere Mechanismus ist mit dem Zusammenwirken der Grundtemperatur und dem Feld der Geschwindigkeitsstörungen verbunden; er erzeugt Störungen, deren Wellenlänge von derselben Größenordnung wie die Schichtdicke ist. Wenn die Temperaturdifferenz quer zur Schicht klein ist, treten Instabilitäten im Fall ausreichend dünner Schichten auf. Für größere Temperaturdifferenzen sind dünne und dicke Schichten instabil, während Schichten von mittlerer Dicke stabil sind. Wenn die Temperaturdifferenz einen bestimmten Wert übersteigt, gibt es keine Schichtdicke, die zu stabilen Bedingungen führt. Diese Ergebnisse, wie auch weitere Aussagen zur Stabilität der Schicht sind in einer sehr klaren Weise unter Verwendung dimensionsloser Parameter ermittelt worden, welche gut geeignet sind, um die theoretischen Ergebnisse mit experimentellen Werten zu vergleichen.

О ТЕРМОКАПИЛЛЯРНЫХ НЕУСТОЙЧИВОСТЯХ В НАГРЕВАЕМОМ СНИЗУ СЛОЕ ЖИДКОСТИ

Аннотация—Исследуется неустойчивость, вызванная термокапиллярными силами у свободной поверхности нагреваемого снизу горизонтального слоя жидкости. Показано существование двух различных механизмов, в соответствии с которыми тепловые эффекты приводят к возникновению дестабилизирующей термокапиллярной силы. Один из них связан с изменением основной температуры за счет деформации свободной поверхности и длинноволновыми возущениями. Другой—с взаимодействием основной температуры с возмущением поля скоростей, и возникающие в этом случае возмущения имеют такой же порядок длины волны, как и глубина слоя. При малой разности температур в слое неустойчивость наблюдается, если слой имеет небольшую глубину. При более существенных разностях температур тонкие и толстые слои являются неустойчивыми, слои же умеренной глубины устойчивы. Когда разность температур превосходит определенное значение, слой не является устойчивым ни при какой глубине. Эти, а также другие результаты, описывающие устойчивость слоя, получены с использованием безразмерных параметров, по которым можно сопоставить теоретические и экспериментальные данные.